Electronic Supplementary Material (ESI) for Journal of Materials Chemistry C.

Supplemental Material

Experimental and theoretical study of β-As_2Te_3 under hydrostatic pressure

R. Vilaplana,[1*] S. Gallego-Parra,[2] E. Lora da Silva,[3] D. Martínez-García,[4] G. Delaizir,[5] A. Muñoz,[6] P. Rodríguez-Hernández[6], V. P. Cuenca-Gotor,[2] J. A. Sans,[2] C. Popescu,[7] A. Piarristeguy,[8] and F. J. Manjón[2]

[1] *Centro de Tecnologías Físicas: Acústica, Materiales y Astrofísica, MALTA Consolider Team, Universitat Politècnica de València, 46022 Valencia, Spain*

[2] *Instituto de Diseño para la Fabricación y Producción Automatizada, MALTA Consolider Team, Universitat Politècnica de València, 46022 Valencia, Spain*

[3] *Institute of Physics for Advanced Materials, Nanotechnology and Photonics, Department of Physics and Astronomy, Faculty of Sciences, University of Porto, 4169-007 Porto, Portugal*

[4] *Departamento de Física Aplicada – ICMUV, MALTA Consolider Team, Universitat de València, Burjassot, Spain*

[5] *Institut de Recherche sur les Céramiques (IRCER), UMR CNRS 7315, Centre Européen de la Céramique, 87068 Limoges, France*

[6] *Departamento de Física, Instituto de Materiales y Nanotecnología, MALTA Consolider Team, Universidad de La Laguna, Tenerife, Spain*

[7] *ALBA-CELLS, Cerdanyola, E-08290 Barcelona, Spain*

[8] *ICGM, Univ Montpellier, CNRS, ENSCM, Montpellier, France*

* Corresponding author E-mail: rovilap@fis.upv.es

Table S1. Experimental (Exp.) and theoretical (Th.) lattice parameters and volume corresponding to the hexagonal unit cell of the *R-3m* structure of β-As_2Te_3 at ambient conditions.

	a (Å)	**c** (Å)	**Volume** (Å^3)
Exp. (sample #1) [a]	4.042(1)	29.463(1)	416.899(4)
Exp. (sample #2) [a]	4.051	29.498	419.225
Th. PBEsol [a]	4.0514	28.50526	405.205
Th. PBE+D3 [a]	4.0940	28.8230	418.460
Exp. [b]	4.047(1)	29.498(2)	418.385(7)
Exp. [c]	4.06	29.59	422.39
Th. PBE [d]	4.062	28.68	409.817
Th. GGA-WC [e]	4.110	29.974	438.49

[a] This work, [b] Ref. S1**,** [c] Ref. S2, [d] Ref. S3**,** [e] Ref. S4

Table S2. Experimental (Exp.) and theoretical (Th.) fractional coordinates corresponding to the *R-3m* phase of β-As_2Te_3 at ambient conditions.

Atoms	Site	Character	x	y	z
Te1	*3a*	Exp. (sample #1) [a]	0	0	0
		Exp. (sample #2) [a]			
		Th. PBE+D3 [a]			
		Th. PBEsol [a]			
		Exp [b]			
		Th. PBE [c]			
Te2	*6c*	Exp. (sample #1) [a]	0	0	0.2153(2)
		Exp. (sample #2) [a]			_
		Th. PBE+D3 [a]			0.21440
		Th. PBEsol [a]			0.21368
		Exp [b]			0.2155(1)
		Th. PBE [c]			0.2140
As	*6c*	Exp. (sample #1) [a]	0	0	0.3979(2)
		Exp. (sample #2) [a]			_
		Th. PBE+D3 [a]			0.39700
		Th. PBEsol [a]			0.39705
		Exp [b]			0.3977(1)
		Th. PBE [c]			0.3967

[a] This work, [b] Ref. S1, [c] Ref. S3

Table S3. Unit-cell volume BM3-EoS data from theoretical (PBE+D3) calculations for β-As_2Te_3, α-Sb_2Te_3, and α-Bi_2Te_3.

Compound	Pressure range (GPa)	V_0 (Å^3)	B_0 (GPa)	B_0'
β- As_2Te_3	0 – 9	418.4(1)	40.1(4)	6.2(3)
α- Sb_2Te_3	0 – 8.9	488.0(1)	35.6(2)	6.1(8)
α- Bi_2Te_3	0 – 8.5	514.5(8)	36.0(1)	6.3(4)

Table S4. Experimental Pressure Coefficients of the four Raman-active frequencies of the tetradymite structure in β-As_2Te_3, α-Sb_2Te_3, and α-Bi_2Te_3.

	β-As_2Te_3	α-Sb_2Te_3	α-Bi_2Te_3
E_g^1	2.5	2.62 [a]	1.96 [b]
A_{1g}^1	4.3	4.5	3.7
E_g^2	0.5	3.6	3.5
A_{1g}^2	1.3	3.0	2.9

[a] Theoretical data from Ref. S5 since there is no experimental data available.
[b] Theoretical data from Ref. S6 since there is no experimental data available.

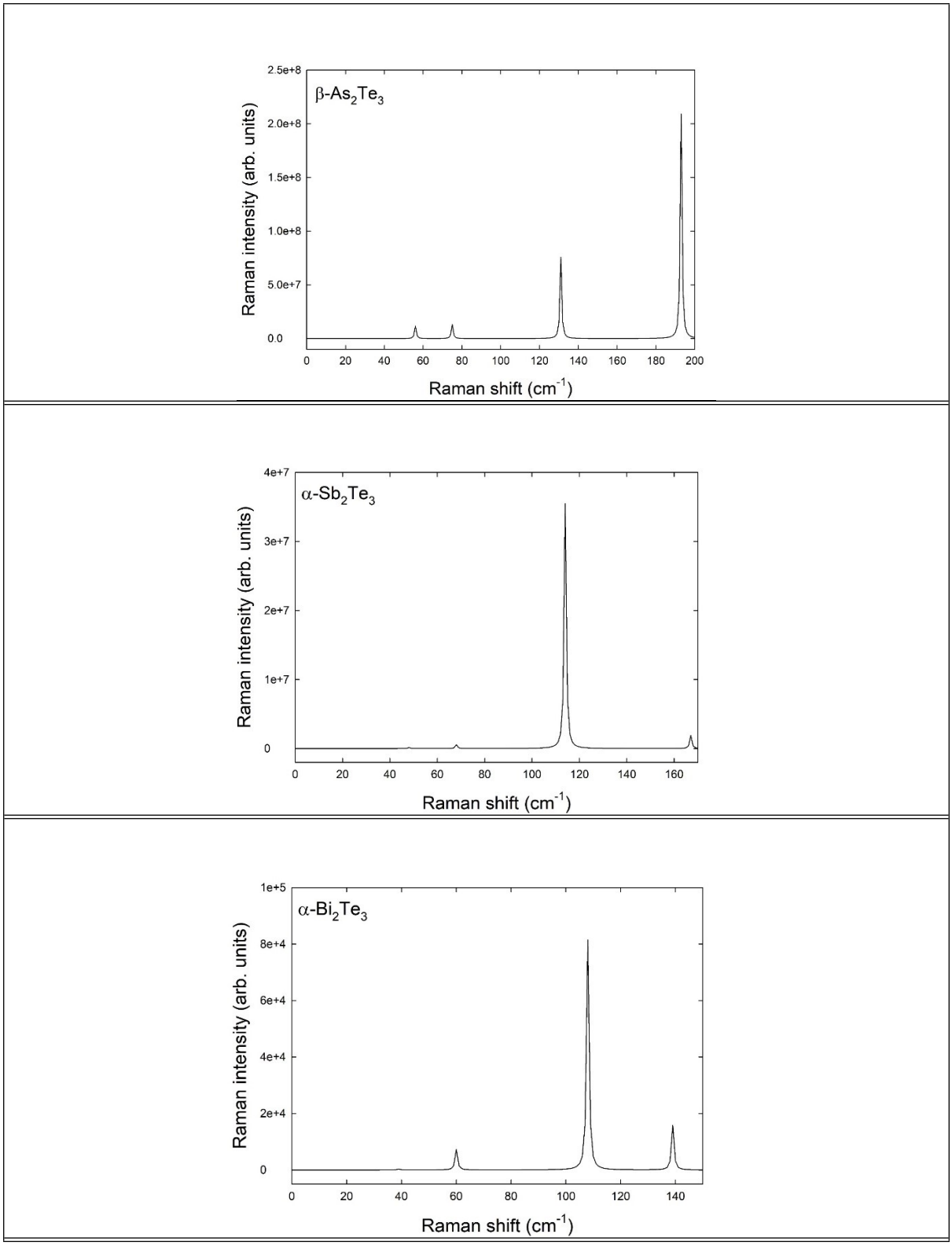

Fig. S1 Simulation of the unpolarized RS spectra of the β-As_2Te_3, | α-Sb_2Te_3 and | α-Bi_2Te_3 at 0 GP a)

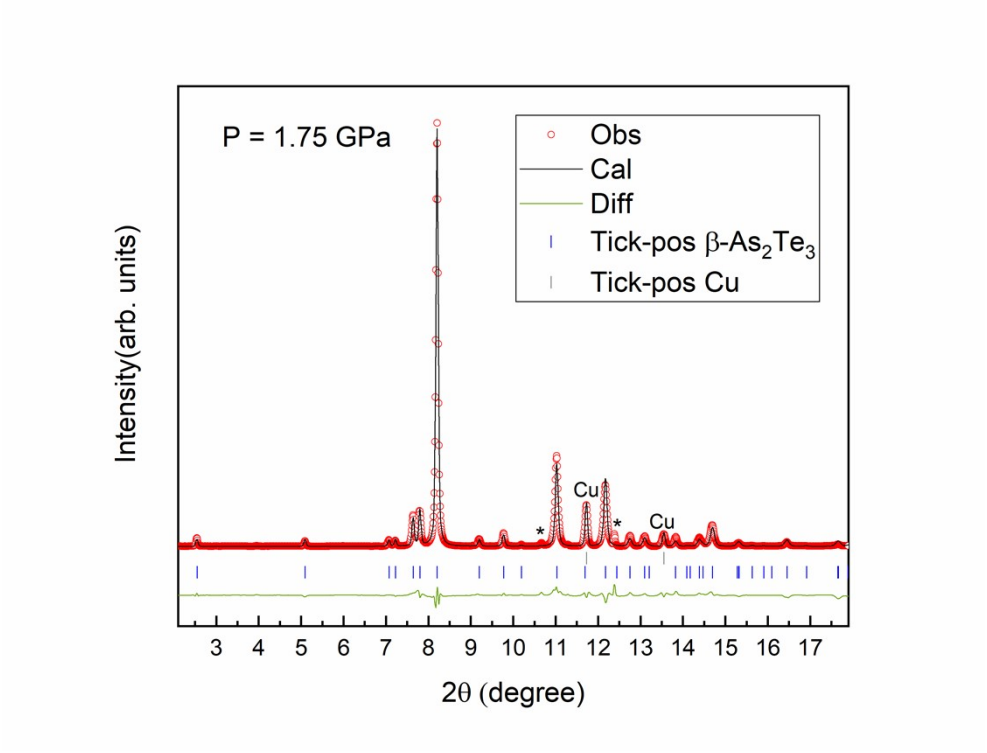

b)

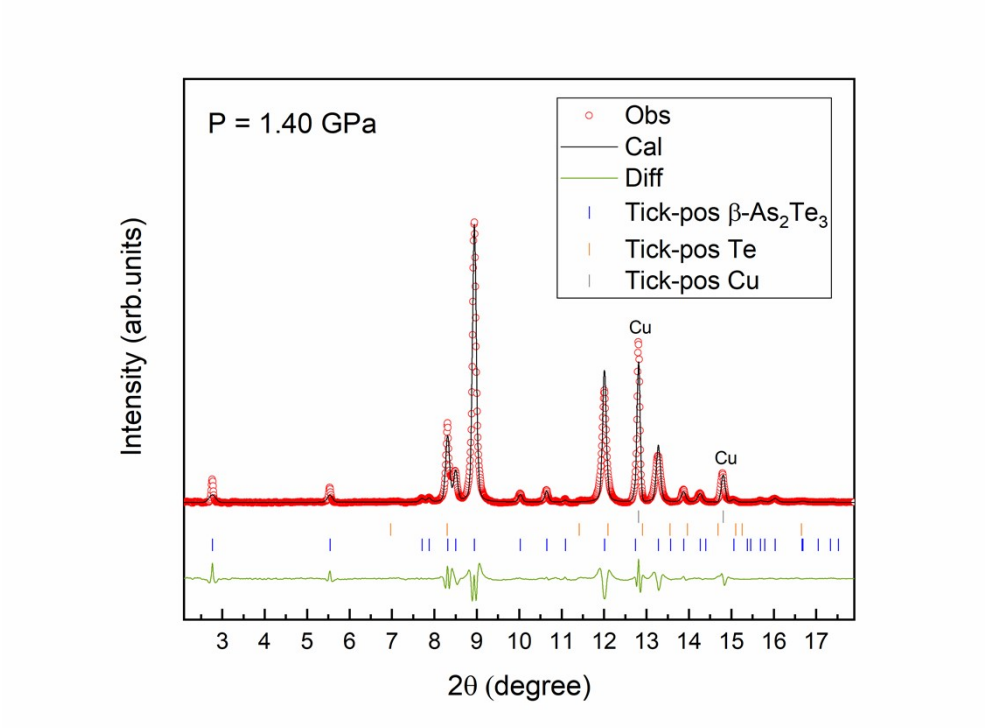

Figs. S2 a) Rietveld refinement of the β phase at 1.75 GPa of sample #1 and b) at 1.40 GPa of sample #2. Experimental data, calculated profiles, and residuals are plotted as solid black lines, red circles, and solid green lines, respectively. The background has been subtracted. Blue, green, and orange vertical ticks indicate the position of Bragg reflections of the β phase, cooper, and Te, respectively.

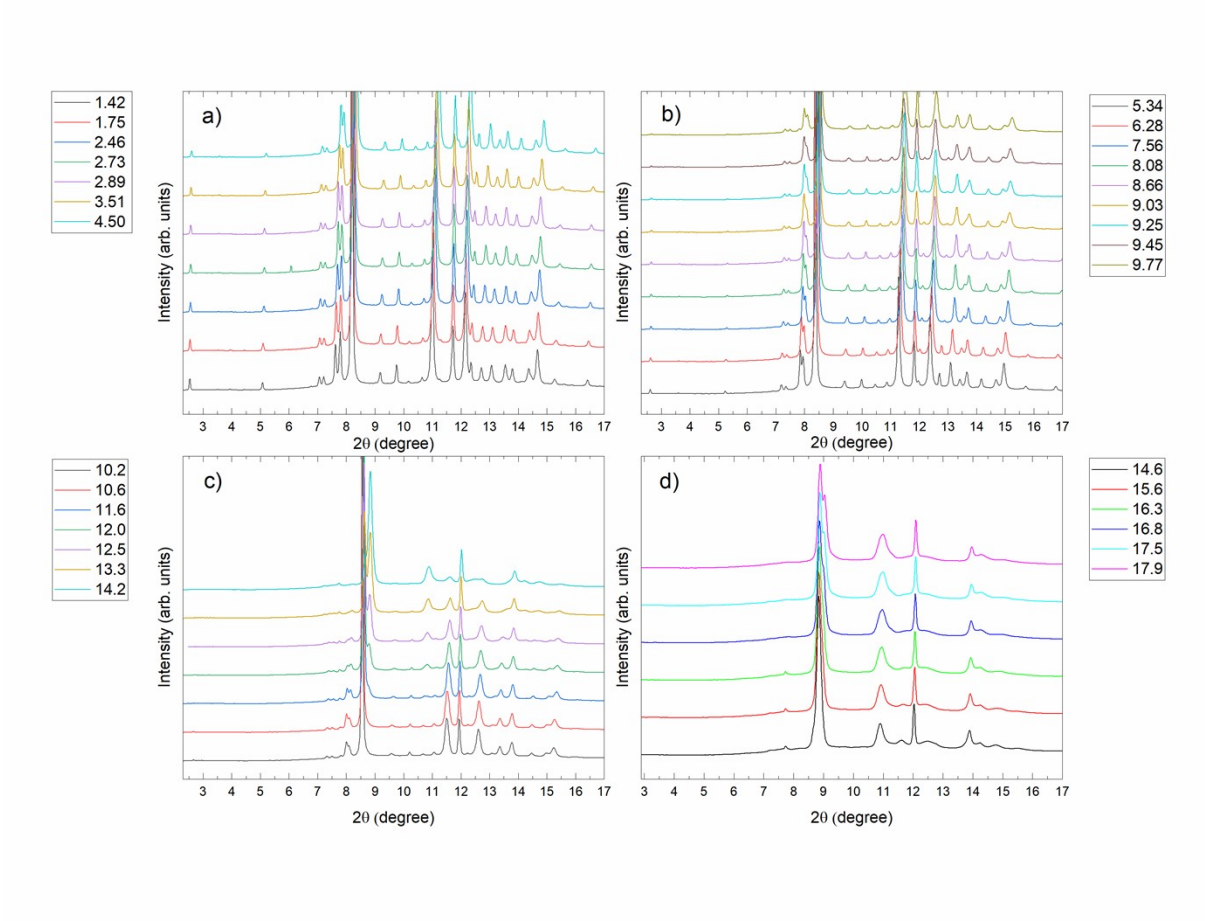

Fig. S3 Experimental diffraction patterns of the experiment with sample #1 of β-As_2Te_3 up to 17.9 GPa. The four plots show the XRD patterns in different pressure ranges, as indicated in the legends.

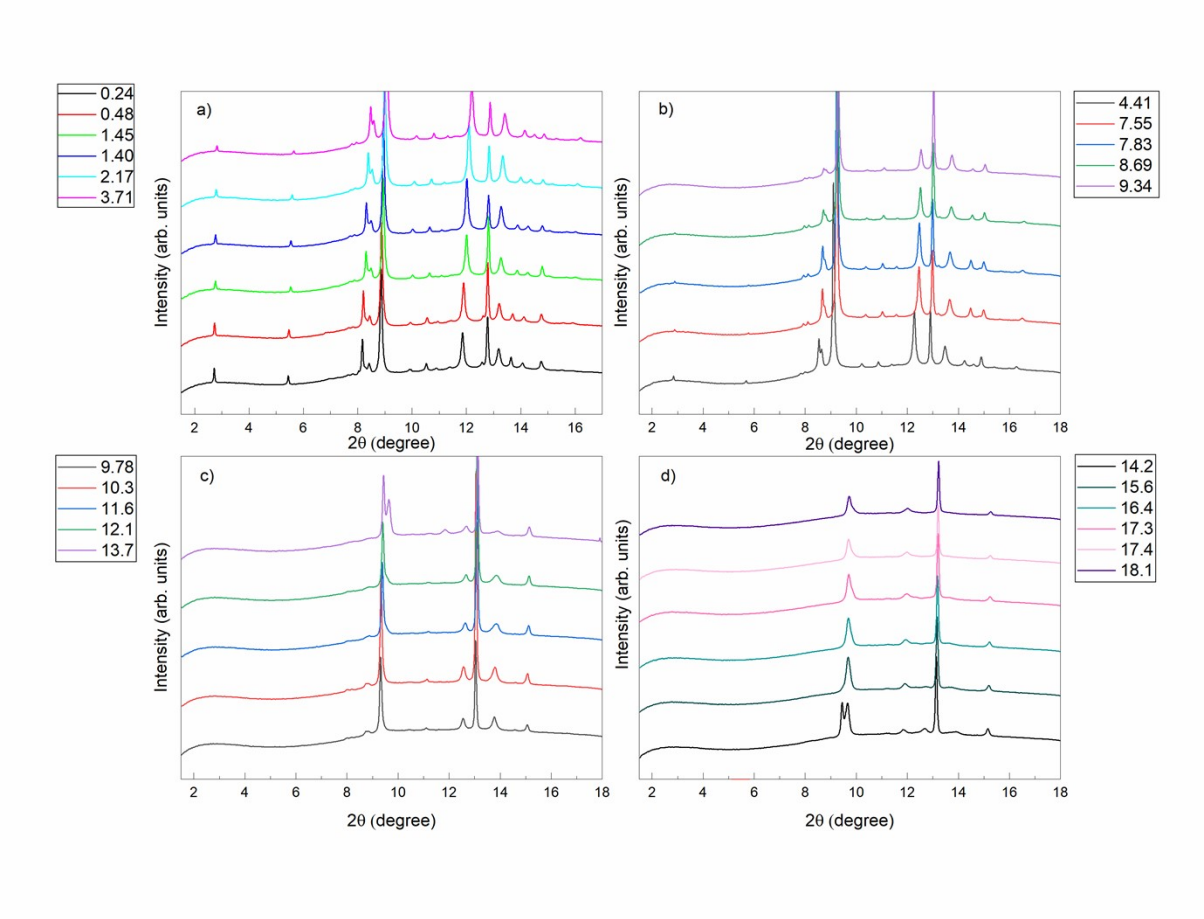

Fig. S4 Experimental diffraction patterns of the experiment with sample #2 of β-As_2Te_3 up to 18.1 GPa. The four plots show the XRD patterns in different pressure ranges, as indicated in the legends.

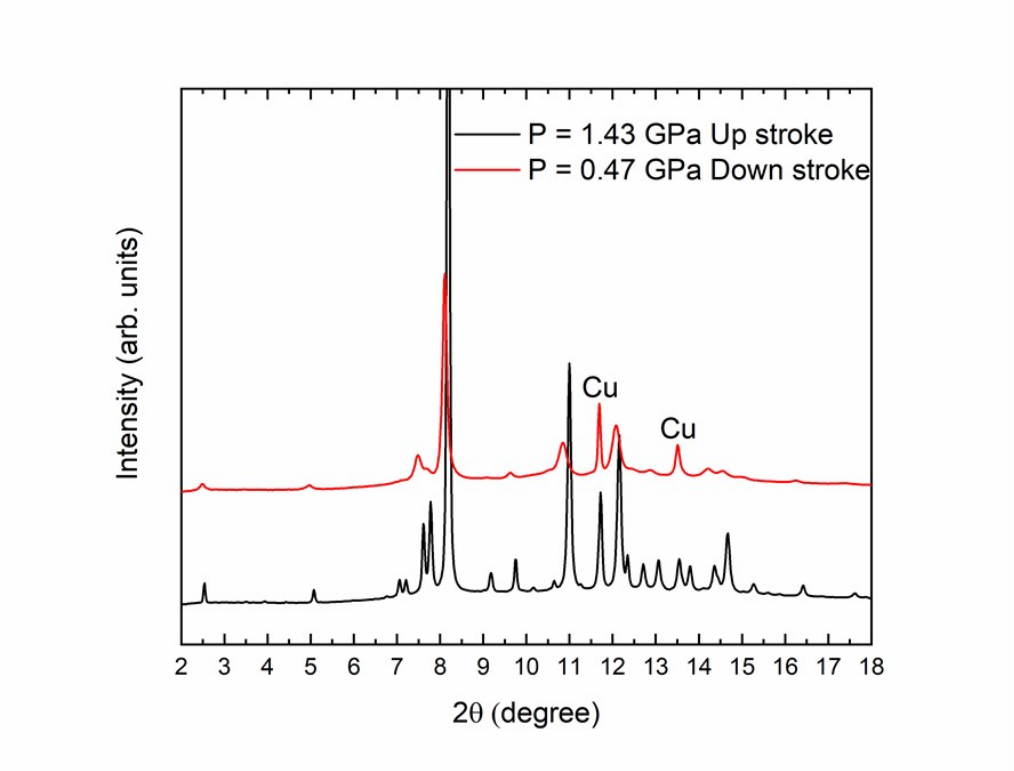

Fig. S5. Experimental XRD patterns of sample #1 of β-As_2Te_3 close to room pressure on upstroke (black color) and downstroke (red color). Copper reflections are indicated.

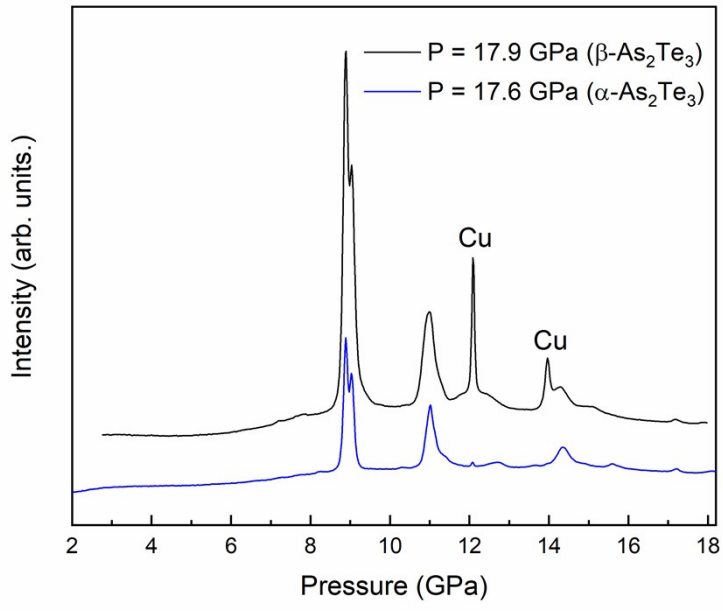

Fig. S6. Experimental XRD patterns of sample #1 of β-As_2Te_3 (black color) and α-As_2Te_3 (blue color) at approximately the same pressure near 18 GPa. Copper reflections are indicated.

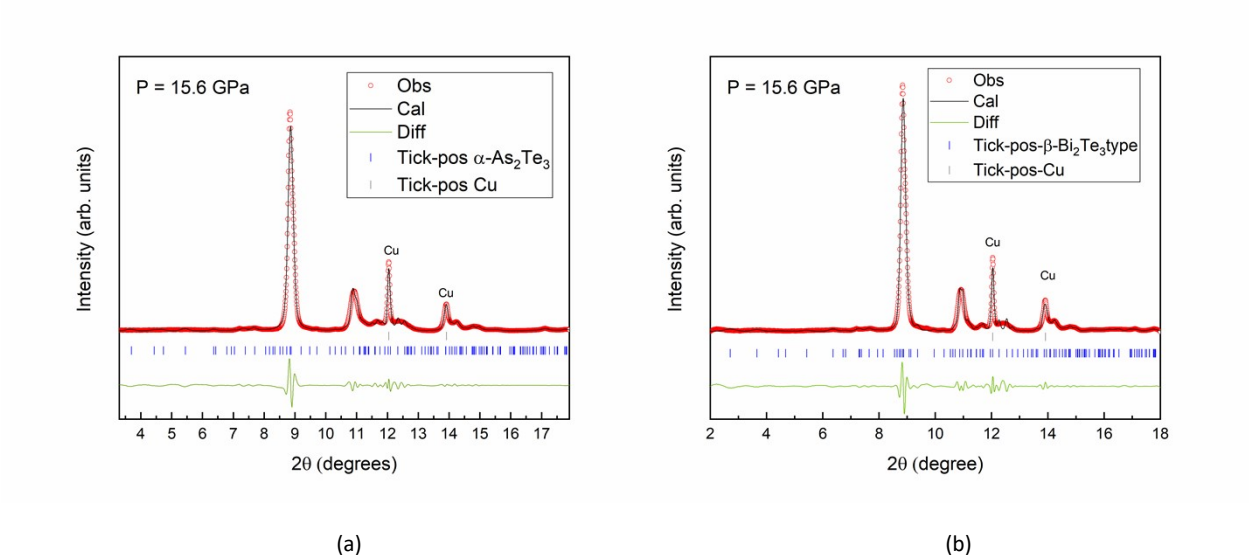

Fig. S7. Le Bail analysis of the diffractogram at 15.6 GPa of sample #1 by using two *C*2/*m* phases such us α-As_2Te_3 (a), and β-Bi_2Te_3 type (b) where the experimental data, calculated profiles and residuals are plotted as black solid lines, red circles and green solid lines, respectively. The background has been subtracted. Black vertical ticks indicate the position of Bragg reflections calculated and the blue ones the position of the cupper reflections.

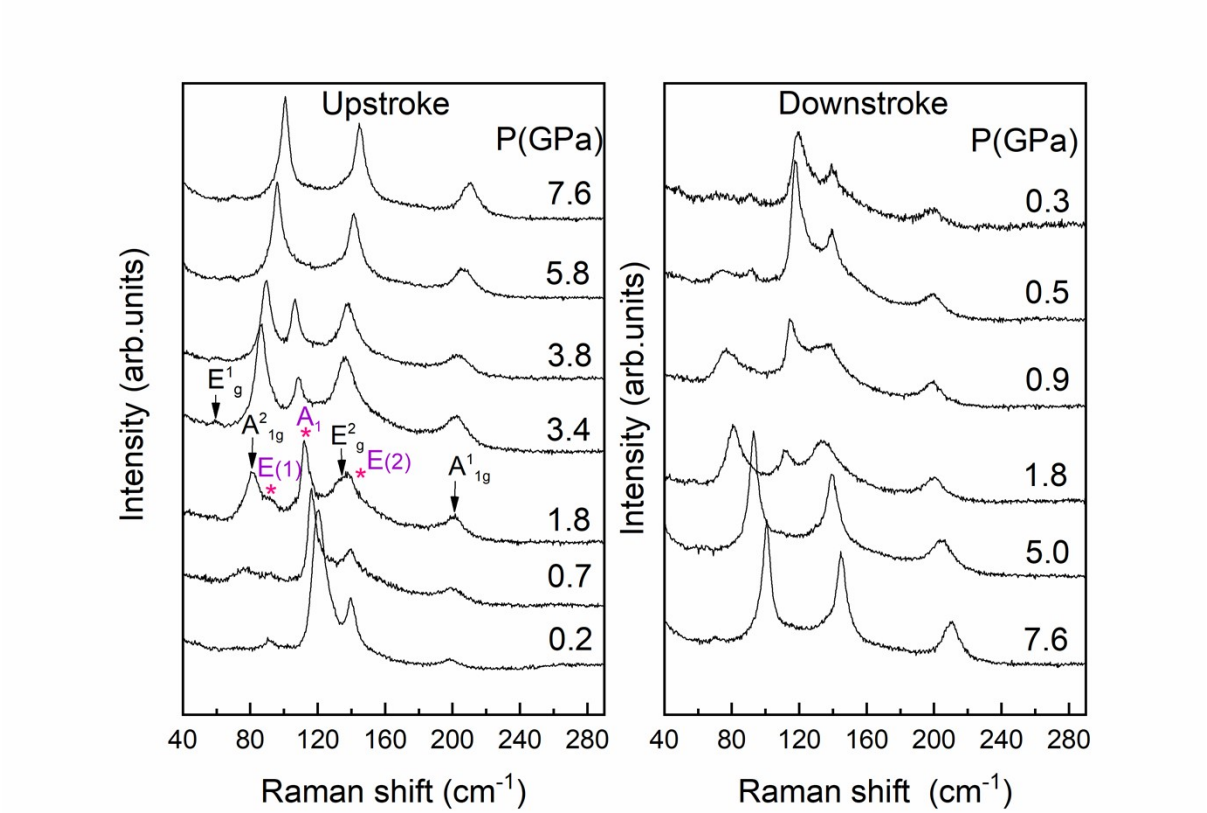

Fig. S8. Upstroke and downstroke experimental Raman spectra of β-As_2Te_3 at different pressures up and from to 7.6 GPa for sample #2, respectively. The four Raman modes are indicated with black arrows and three modes of the tellurium with magenta asterisks

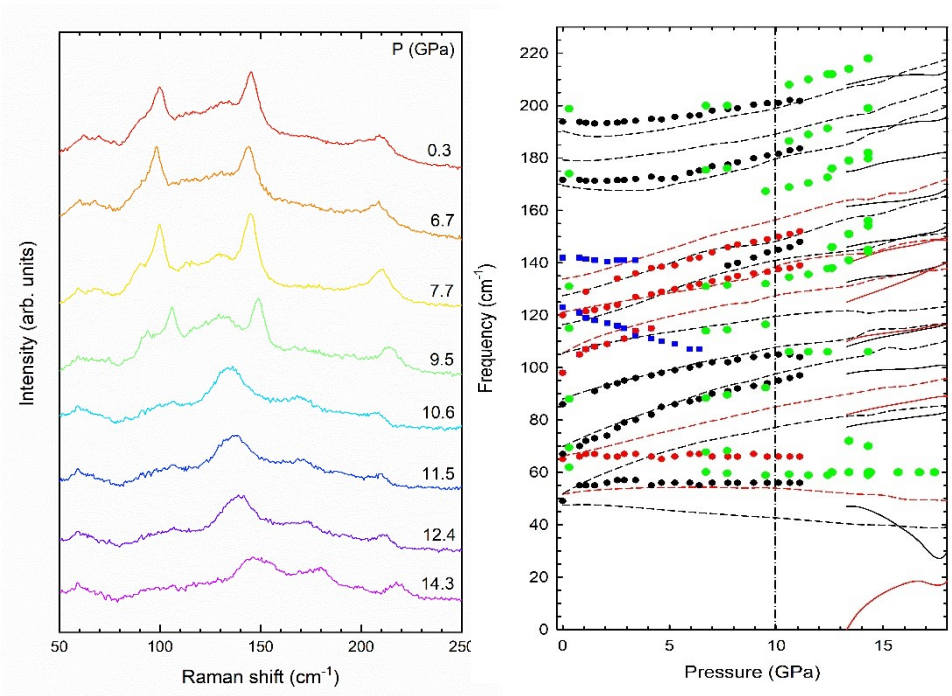

Fig. S9. (a) Downstroke of sample #1 from 14.3 GPa to 0.3 GPa. (b) Pressure dependence of the Raman frequencies of the broad bands of (a) on downstroke (green circles). They can be compared to experimental Raman modes of α-As_2Te_3 (black and red circles taken from Ref. S7) as well as with theoretical (PBE+D3) frequencies for α-As_2Te_3 (dashed lines) and for the β-Bi_2Te_3 phase of As_2Te_3 (solid lines above 13.3 GPa). The vertical dashed dotted line indicates the pressure at which the HP phase reverts to the low-pressure phase.

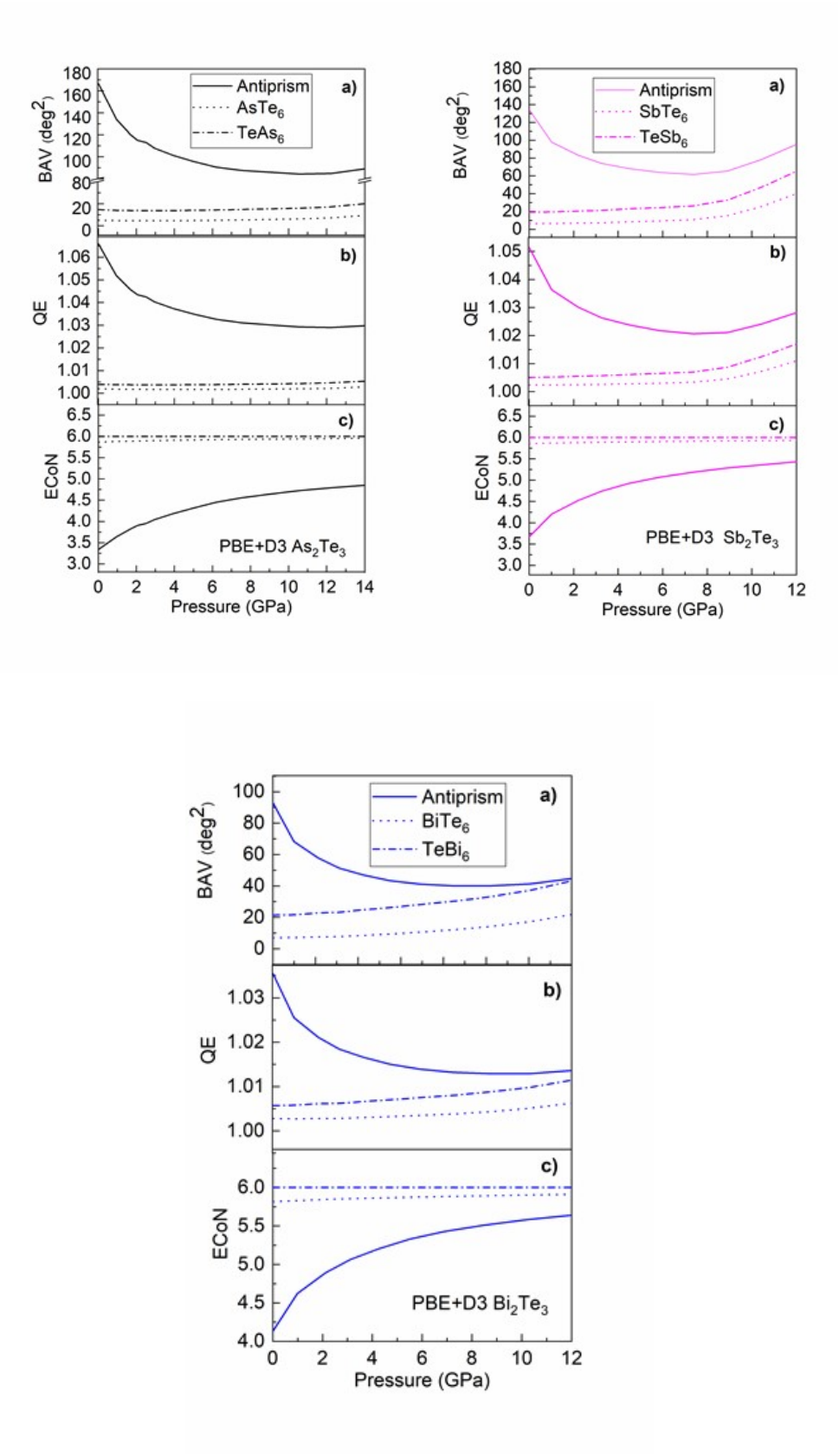

Fig. S10. Theoretical (PBE+D3) pressure dependence of the bond angle variance (BAV) (a), quadratic elongation (QE) (b), and effective coordination number (ECoN) (c) of the XTe_6 and TeX_6 octahedrons and of the octahedron associated with the antiprism for β-As_2Te_3, α-Sb_2Te_3 and α-Bi_2Te_3 in black, magenta and blue colors, respectively.

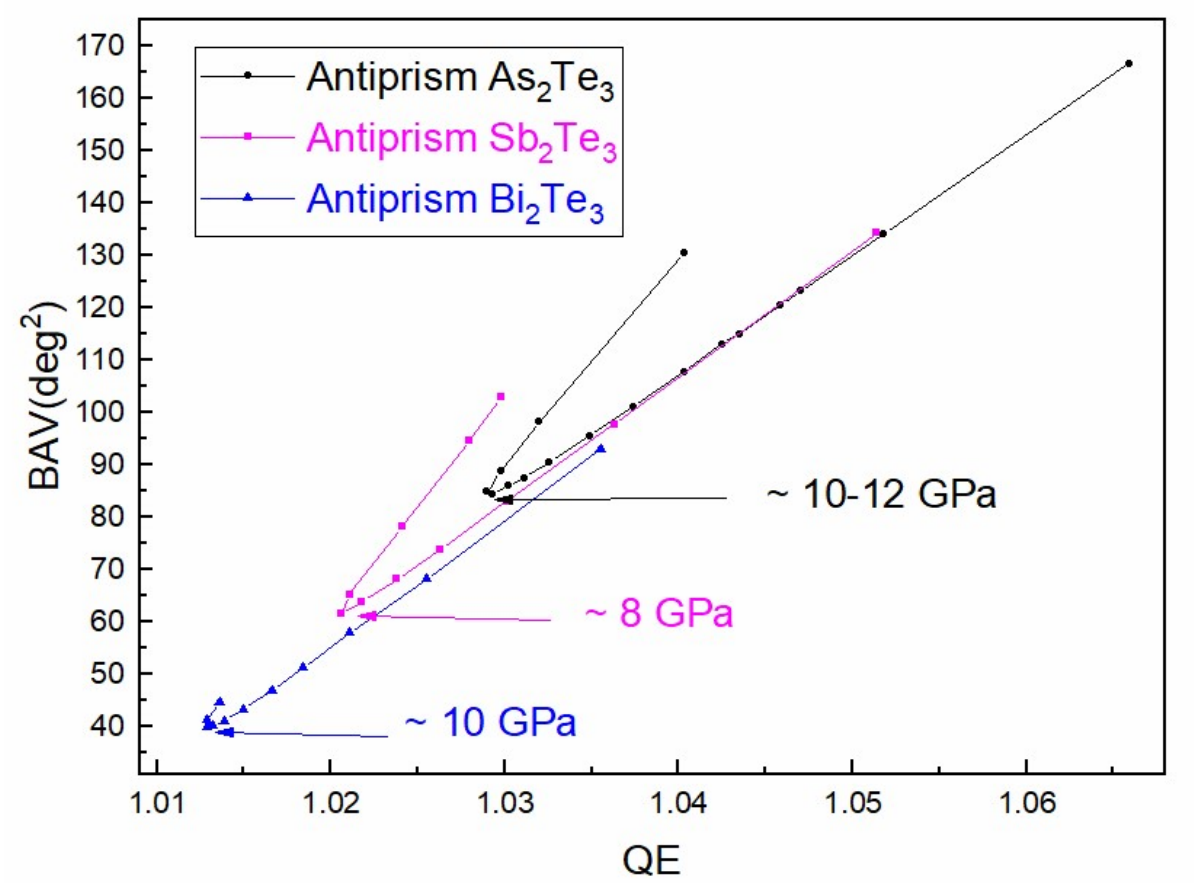

Figure S11. Bond angle variance (BAV) vs. quadratic elongation (QE) of the Te2 antiprism in β-As_2Te_3, α-Sb_2Te_3, and α-Bi_2Te_3. The pressure at which we observed slope changes are indicated with arrows.

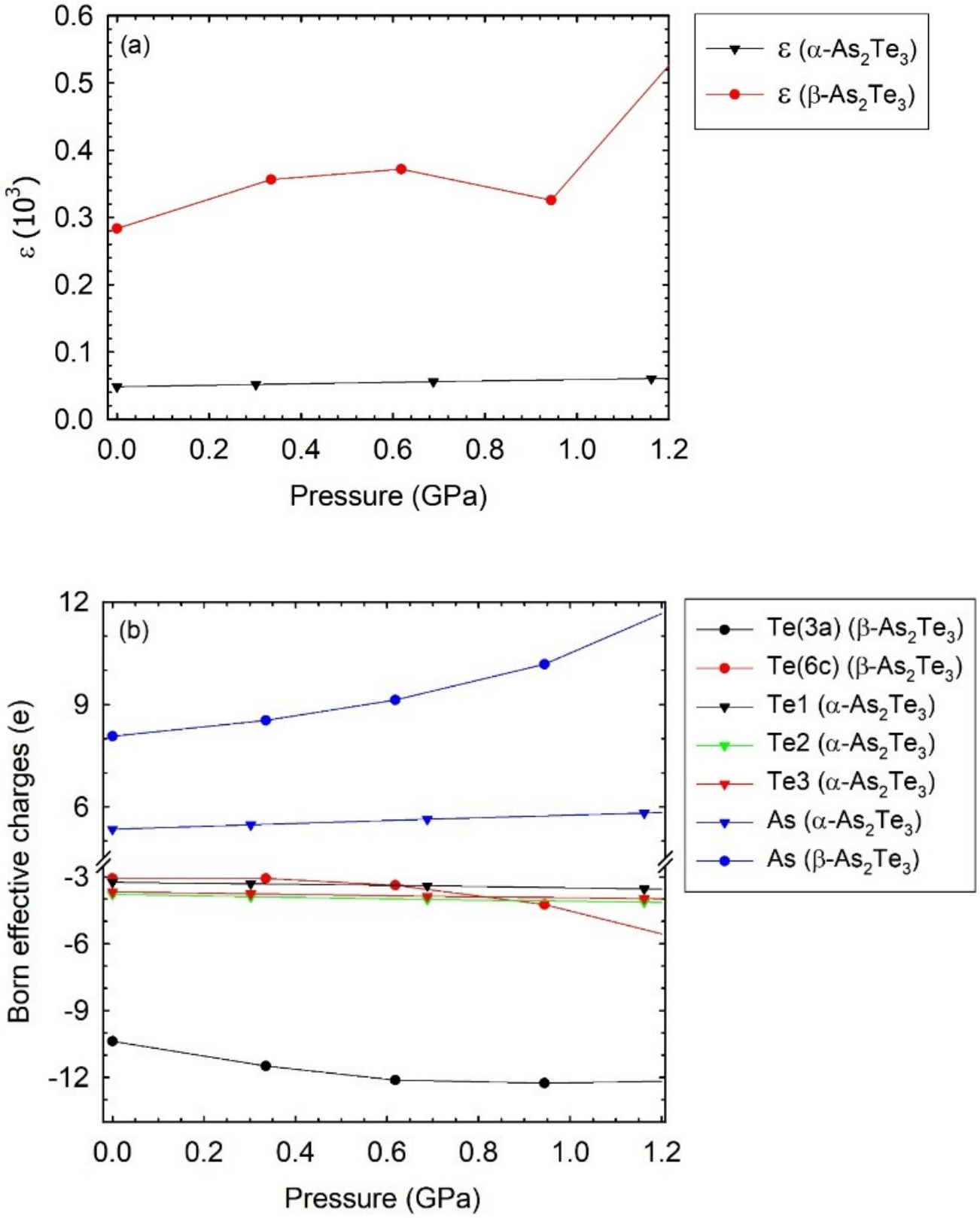

Fig. S12. Theoretical (PBE+D3) pressure dependence of the optical dielectric constant (a) and Born effective charges (b) in β-As_2Te_3 and α-As_2Te_3.

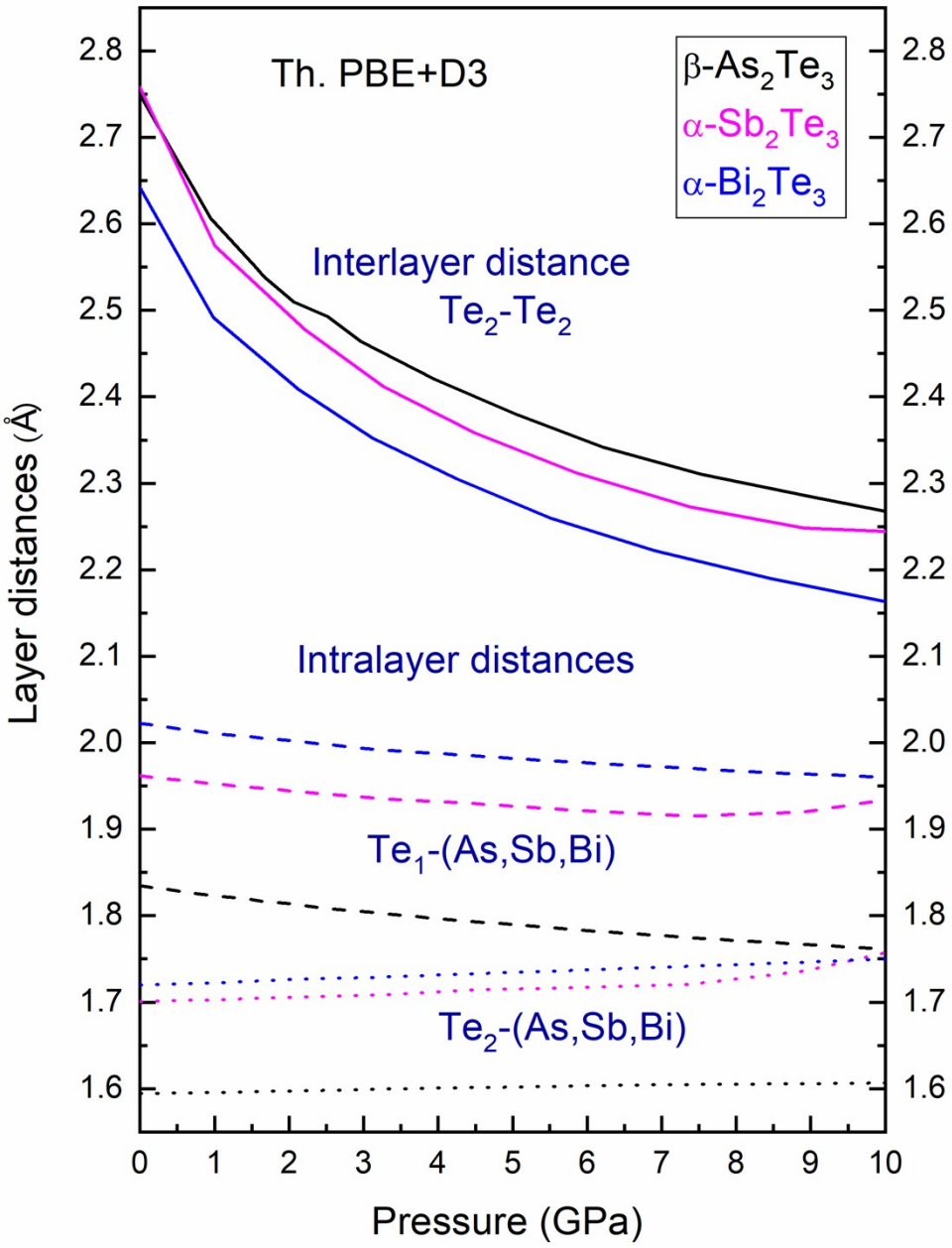

Fig. S13. Pressure dependence of the theoretical (PBE+D3) interlayer and intralayer distances for isostructural β-As_2Te_3, α-Sb_2Te_3 and α-Bi_2Te_3. The continuous, dashed, dash-dotted lines indicate the interlayer distance Te2-Te2 and the intralayer distances Te1-(As, Sb, Bi) and Te2-(As, Sb, Bi), respectively. Note that values of α-Sb_2Te_3 above 7.5 GPa are not reliable because of problems in the relaxation of the *R-3m* structure of this compound above that pressure.

References

S1. Morin, C.; Corallini, S.; Carreaud, J.; Vaney, J.-B.; Delaizir, G.; Crivello, J.-C.; Lopes, E. B.; Piarristeguy, A.; Monnier, J.; Candolfi, C. Polymorphism in thermoelectric As2Te3. *Inorganic chemistry* **2015**, *54*, 9936-9947.

S2. Shu, H. W.; Jaulmes, S.; Flahaut, J. Systeme As/1bTe-Mise en evidence et etude structurale d'une nouvelle variete de As2Te3 metastable. *Materials research bulletin* **1986**, *21*, 1509-1514.

S3. Deng, H. Theoretical prediction of the structural, electronic, mechanical and thermodynamic properties of the binary α-As2Te3 and β-As2Te3. *Journal of Alloys and Compounds* **2016**, *656*, 695-701.

S4. Sharma, Y.; Srivastava, P. First principles investigation of electronic, optical and transport properties of α-and β-phase of arsenic telluride. *Optical Materials* **2011**, *33*, 899-904.

S5. Gomis, O.; Vilaplana, R.; Manjón, F.; Rodríguez-Hernández, P.; Pérez-González, E.; Muñoz, A.; Kucek, V.; Drasar, C. Lattice dynamics of Sb 2 Te 3 at high pressures. *Physical Review B* **2011**, *84*, 174305.

S6. Vilaplana, R.; Gomis, O.; Manjón, F.; Segura, A.; Pérez-González, E.; Rodríguez-Hernández, P.; Muñoz, A.; González, J.; Marín-Borrás, V.; Muñoz-Sanjosé, V. High-pressure vibrational and optical study of Bi 2 Te 3. *Physical Review B* **2011**, *84*, 104112.

S7. Cuenca-Gotor, V. P.; Sans, J.; Ibáñez, J.; Popescu, C.; Gomis, O.; Vilaplana, R.; Manjón, F.; Leonardo, A.; Sagasta, E.; Suárez-Alcubilla, A. Structural, vibrational, and electronic study of α-As2Te3 under compression. *The Journal of Physical Chemistry C* **2016**, *120*, 19340-19352.